ANNALS of Faculty Engineering Hunedoara – International Journal of Engineering
ISSN 1584 - 2665 (printed version); ISSN 2601 - 2332 (online); ISSN-L 1584 - 2665

[1.]Ashish BALDANIA, [2.]Vibhute BHALCHANDRA, [3.]Sachin PARIKH

SYNTHESIS OF ACTIVATED CARBON FROM BIOMASS

[1,2.]Faculty of Technology, R.K. University, Rajkot, INDIA
[3.]Chemical Engineering Department, L.D. Engineering College, Ahmedabad, INDIA

Abstract: Activated carbon is unique and versatile adsorbents having extended surface area, micro porous structure, universal adsorption effect, high adsorption capacity and high degree of surface reactivity. Activated carbons are synthesized from variety of materials. Most commonly used on a commercial scale are cellulosic based precursors such as peat, coal, lignite, wood and coconut shell. Variation occurs in precursors in terms of structure and carbon content. Pine Wood is found to be one of the valuable raw materials for the production of highly porous activated carbon and other important factor is its high carbon content. Exploration of good low cost and non–conventional adsorbent may contribute to the sustainability of the environment and offer promising benefits for the commercial purpose in future. Pyrolysis is carried out in absence of oxygen and under the vacuum condition to enhance the surface area and to develop interconnecting porosity. Activated carbon produced from biomass is cost effective as it is easily available as a waste biomass. Activated carbon produced by pyrolysis process has higher surface area of 969.075 m^2/g.

Keywords: Activated Carbon, Pyrolysis, Pine Wood, Biomass, Surface Area, Porosity

1. INTRODUCTION

Biomass is the most abundantly available raw material on the Earth for the production of bio–fuels, mainly bio–ethanol. It is composed of carbohydrate polymers (cellulose, hemicellulose), and an aromatic polymer (lignin). These carbohydrate polymers contain different sugar monomers (six and five carbon sugars) and they are tightly bound to lignin. Waste biomass is produced as a low value by-product of various industrial sectors such as agricultural (sugarcane bagasse, straw etc.), forestry (saw mill and paper mill discards). Energy crops are crops with high yield of biomass produced to serve as a raw material for production of second generation biofuel examples include grass. Both the cellulose and hemicellulose fractions are polymers of sugars, and thereby a potential source of fermentable sugars, or other processes that convert sugars into products. Hemicellulose can be readily hydrolysed under mild acid or alkaline conditions. The cellulose fraction is more resistant and therefore requires more rigorous treatment. [2,4,30].

— Cell wall of plants

Different plant species and different developmental stages of the plant, tissues and cells vary in the structure and composition of the plant cell wall. A differentiation in the plant cell walls is made in the primary wall layer, a flexible layer which is formed as the cell is still capable of growing. During the cell formation the middle lamella and primary wall are formed first. The subsequent cell– thickening is onset when the bulk of cellulose and hemicellulose are deposited in the secondary wall. The secondary wall layer, which is formed after the cell is fully grown; and the middle lamella gluing the plant cells. The plant cell wall is highly organized and contains networks of polysaccharides, proteins and aromatic substances. The cell walls form the exterior of the plasma membrane and serve multiple purposes. They prevent membrane rupture, are involved in cell size and shape determination and control the rate and direction of cell growth. By providing rigidity to the plant cells, the walls function as the skeleton of the plant. The quantity of the main components of wood differs if it is softwood or hardwood. [22,23].

— Cell wall composition

The secondary cell wall is composed of the carbohydrate polymers cellulose and hemicellulose, lignin and some minor components, like proteins and minerals. Biomass typically contains 55–75% (w/w) of polysaccharides, built–up of various pentose and hexose units. [22,23].

— Hemicellulose

Hemicelluloses are the second major components of plant cell walls, which are found in the primary and secondary cell walls of land and fresh water plants, and in some seaweed. It's a group of heterogeneous polysaccharides. Hemicelluloses are associated with cellulose and are usually a mixture of monosaccharide such as D–xylose, L–arabinose, D–glucose, D–galactose, D–mannose, D–glucuronic acid, 4–O–methyl–D–glucuronic acid and D–galacturonic and to minor amount of L–rhamnose, L–fructose and a variety of O–methylated neutral sugars. These complex polysaccharides are non–crystalline polymers and form hydrogen bonds with cellulose and covalent bonds with lignin. Hemicelluloses differ from cellulose not only in crystalline aspect but also in Degree of Polymerization (about 100 in softwoods and about 200 in hardwoods) and in molar mass, being significantly lower for hemicelluloses. Their general formula is $(C_5H_8O_4)$ n for a pentosan and $(C_9H_{10}O_5)$ n for a hexosan. Considerable differences exist in hemicellulose composition and structure between softwood and hardwood. Hardwood contains mostly Xylan, whereas softwood contains mostly galactoglucomannans. Softwood Xylan cannot be directly extracted with alkali as it is necessary to first delignify the cellulose. Some studies on utilization of hemicellulose have demonstrated that they are potentially very useful. The hemicelluloses extracted from wheat straw have the ability to serve as adhesives also as thickeners and emulsifiers in food. [20,22,23].

— Xylan

The most abundant hemicelluloses in nature are xylan. Xylan is the main hemicellulose components of secondary cell walls constituting about 10–30% of the biomass of hardwoods and herbaceous plants. In some tissues of grasses and cereals Xylan can constitute up to 50% of the biomass. Xylan comprise a β– (1→4)–D–xylopyranose backbone, which can be substituted with short carbohydrate chains based on L–arabinose, 4–O–methyl–D–glucuronic acid, D or L–galactose or D–glucuronic acid. The botanical source strongly determines the specific features with respect to type, amount, position and distribution of substituent over the xylan backbone. Xylan containing few substituents tends to self–associate, forming aggregates with a low solubility. [20,22].

— Xylose

Xylose is a sugar first isolated from wood, and named for it. Xylose is classified as a monosaccharide of the aldopentose type, which means that it contains five carbon atoms and includes a formyl functional group. It is derived from hemicellulose, one of the main constituents of biomass. Like most sugars, it can adopt several structures depending on conditions. With its free carbonyl group, it is a reducing sugar. The acyclic form of xylose has chemical formula $HOCH_2(CH(OH))_3CHO$. The cyclic hemiacetal isomers are more prevalent in solution and are of two types: the pyranoses, which feature six–member C_5O rings, and the furanoses, which feature five–member C_4O rings (with a pendant CH_2OH group). Each of these rings subject to further isomerism, depending on the relative orientation of the anomeric hydroxy group. Xylose is the main building block for the hemicellulose xylan, which comprises about 30% of some plants (birch for example) far less in others (spruce and pine have about 9% xylan). Xylose is otherwise pervasive, being found in the embryos of most edible plants. [20,22,23].

— Activated carbon

The first known use of activated carbon dates back to the Ancient Egyptians who utilized its adsorbent properties for purifying oils and medicinal purposes. Centuries later, the early ocean–going vessels stored drinking water in wooden barrels, the inside of which had been charred. (However, by modern definition the carbon used in these applications could not truly be described as "activated"). Granular activated carbon was used to this end as, indeed, it still is today. By the late 1930's there was considerable industrial–scale use of carbon for gaseous and liquid phase application and new manufacturing processes had been developed to satisfy the needs of industry. During the 1939–1945 war, a further significant development took place – the production of more sophisticated chemically impregnated carbon for entrapment of both war and nerve gases. Modern day uses of carbon are diverse, to say the least. It is also used in consumer products such as refrigerator deodorizers and at the other end of the spectrum in high technology applications such as nuclear power plant containment systems. [1,3,5].

The most commonly used raw materials are coal (anthracite, bituminous and lignite), coconut shells, wood (both soft and hard), peat and petroleum based residues. Many other raw materials have been evaluated such as walnut shells, peach pits and palm kernels but invariably their commercial limitation lies in raw material supply. This is illustrated by considering that 1,000 tons of untreated shell type raw materials will only yield about 100 tons of good quality activated carbon. Most carbonaceous materials do have a certain degree of porosity and an internal surface area in the range of 10–15 m^2/g. During activation, the internal surface becomes more highly developed and extended by controlled oxidation of carbon atoms – usually achieved by the use of steam at high temperature. After activation, the carbon will have acquired an internal surface area between 700 and 1,200 m^2/g, depending on the plant operating conditions. The internal surface area must be accessible to the passage of a fluid or vapor if a potential for adsorption is to exist. Thus, it is necessary that an activated carbon has not only a highly developed internal surface but accessibility to that surface via a network of pores of differing diameters. As a generalization, pore diameters are usually categorized as follows: [25,27].

Micro pores <40 °A
Mesopores 40 – 5,000 °A
Macro pores >5,000 °A (typically 5000–20000 °A)

During the manufacturing process, macro pores are first formed by the oxidation of weak points (edge groups) on the external surface area of the raw material. Mesopores are then formed and are, essentially, secondary channels formed in the walls of the macro pores structure. Finally, the micro pores are formed by attack of the planes within the structure of the raw material. All activated carbons contain micro pores, meso pores, and macro pores within their structures but the relative proportions vary considerably according to the raw material. A coconut shell based carbon will have a predominance of pores in the micro pores range and this account for 95% of the available internal surface area. In contrast wood and peat based carbons are predominantly meso/macro pores structures and are, therefore, usually suitable for the adsorption of large molecular species. Such properties are used to advantage in decolorization processes. Coal based carbons, depending on the type of coal used; contain pore structures somewhere between coconut shell and wood. In general, it can be said that macro pores are of little value in their surface area, except for the adsorption of unusually large molecules and are, therefore, usually considered as an access point to micro pores. Mesopores do not generally play a large role in adsorption, except in particular carbons where the surface area attributable to such pores is appreciable (usually 400 m^2/g or more). Thus, it is the micro pores structure of an activated carbon that is the effective means of adsorption. It is, therefore, important that activated carbon not be classified as a single product but rather a range of products suitable for a variety of specific applications. [10,12,28,31].

2. MATERIALS AND EXPERIMENTAL METHODS

— Materials

Waste Pine Wood is collected from, Krishna Vijay Saw Mill, Bhuj and is screened with 100 mesh size sieve Figure [1,2]. Biomass Material (Pine Wood) is preserved into polyethylene bags till the use in to laboratory [6,14,].

Figure 1. Furniture Waste for Experiment (Pine Wood – Biomass)

Figure 2. Sieved Pine Wood for Pyrolysis Process

— Experimental methods

To know the upper use temperature of a material (Pine Wood) TGA is being carried out. Beyond this temperature the material will begin to degrade. Thermo gravimetric analysis (TGA) is an analytical technique used to determine a material's thermal stability and its fraction of volatile components by monitoring the weight change that occurs as a sample is heated at a constant rate. As per the data calculation temperature of Pine wood is 550°C. Pyrolysis process is being carried out to synthesis the Activated Carbon from Pine Wood. With the help of Pyrolysis process in the absence of air and under the vacuum condition the experiment is carried out for three different temperatures (500°C, 550°C and 600°C). A defined amount (25 gm) of Pine wood is taken in to the vessel and heated up to 2 hrs after the desired temperature is reached Figure [3]. The resultant product is then analyzed for elemental analysis, powder X – Ray diffraction, surface area – porosity measurement (BET), particle size analysis and field emission scanning electron microscope (SEM). [18,19,26,29].

Figure 3. Pyrolysis Process of Pine Wood under the Vacuum Condition

3. RESULTS AND DISCUSSION

— Elemental Analysis

Elemental analysis is a process where a sample of material is analyzed for its elemental and isotopic composition. Data shows increase in temperature with decrease in % moisture content. Sample which is taken (for 550°C) is having highest amount of % fixed carbon. Similarly, decrease in % volatile matter with increase in temperature Table [1]. Highest amount of % Ash Content present at Sample (for 600°C) [7,8,24].

— X– Ray powder diffraction (XRD)

X–ray powder diffraction (XRD) is a rapid analytical technique primarily used for phase identification of a crystalline material and can provide information on unit cell dimensions. The analyzed material is finely ground, homogenized, and average bulk composition is determined Figure [4–7]. As per the Results Table [2] and Graphs higher weight % of C Element is present for 550°C Sample. [7,8,24].

Table 1. Elemental Analysis of Raw Material and Activated at Various Temperatures

Sample ID	Weight of Sample (gm)	% Moisture Content	% Ash Content	% Volatile Matter	% Fixed Carbon
Pine Wood	1.00	5.68	20.57	62.30	11.45
for 500°C	1.00	3.23	57.89	17.82	21.06
for 550°C	1.00	2.74	41.65	15.44	40.17
for 600°C	1.00	2.18	62.53	12.19	23.10

Table 2. XRD Weight % of Elements for Raw Material and Activated Carbon at Various Temperatures

Sample ID	Weight % of Element		
	Element C	Element O	K and Other Element
Pine Wood	60.77	38.96	0.27
for 500°C	69.48	19.79	10.73
for 550°C	89.33	6.41	4.26
for 600°C	83.04	14.82	2.14

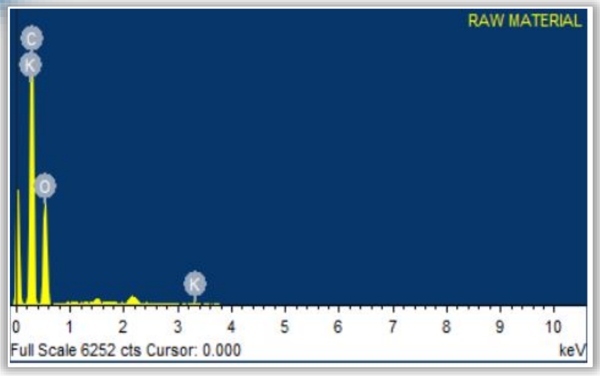

Figure 4. X – Ray Diffraction graph of Pine Wood

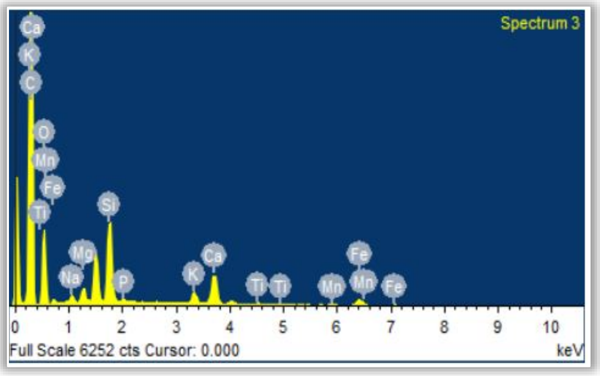

Figure 5. X – Ray Diffraction graph of Activated Carbon at 500ºC

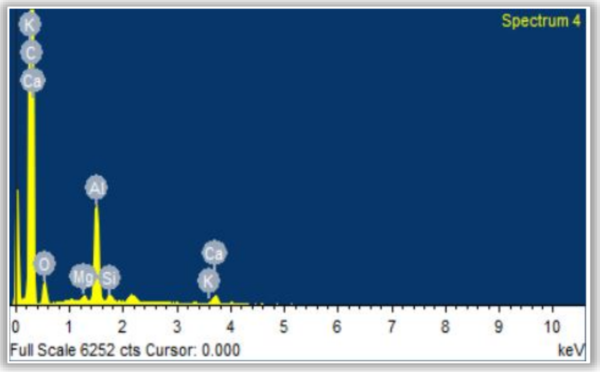

Figure 6. X – Ray Diffraction graph of Activated Carbon at 550ºC

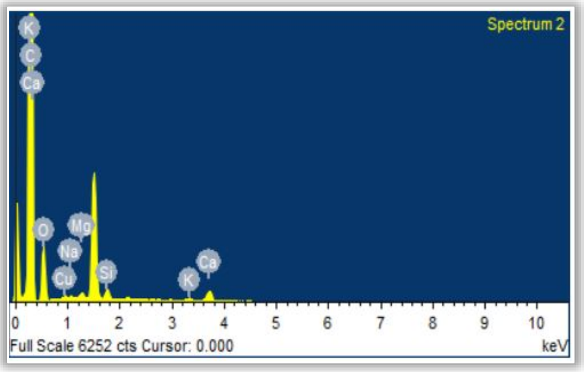

Figure 7. X – Ray Diffraction graph of Activated Carbon at 600ºC

— Surface area and Porosity measurement (BET)

By BET (Brunauer, Emmett and Teller) the specific surface area of a sample is measured, including the pore size distribution. The specific surface determined by BET relates to the total surface area (reactive surface) as all porous structures adsorb the small gas molecules. Porosity is a measure of the void (i.e. "empty") spaces in a material over the total volume. As per the data Table [3] and Isotherm Linear Plot Figure [8–10] at 550ºC, highest Surface area 969.075 m^2/g is achieved with Pore volume of 0.56 cm^3/g. [9,11,13].

Table 3. Result of BET Surface Area and Pore Volume of Activated Carbon at Various Temperature

Sr. No.	Temperature (ºC)	BET Surface Area (m^2/g)	Single Point Adsorption total pore volume of Pores < 1,934,646 ºA (cm^3/g)
1	500ºC	546.265	0.043847
2	550ºC	969.075	0.056302
3	600ºC	850.083	0.050828

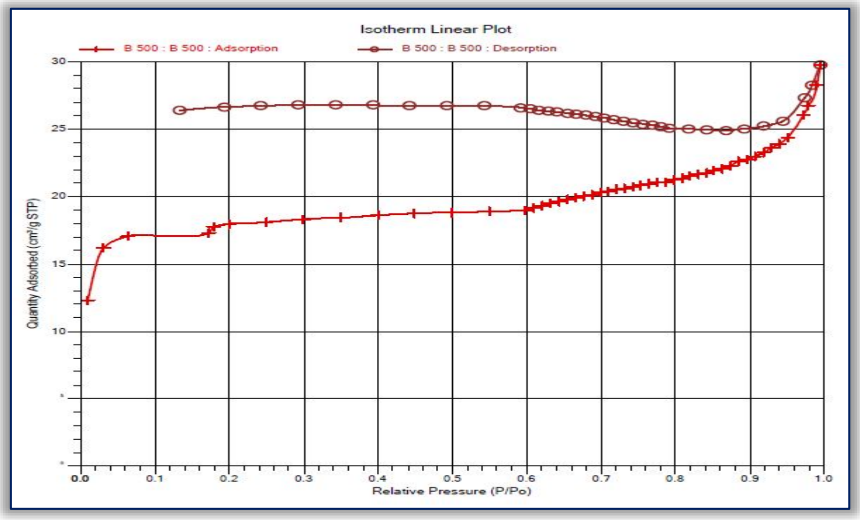

Figure 8. Isothermal Linear Plot of Activated Carbon at 500ºC

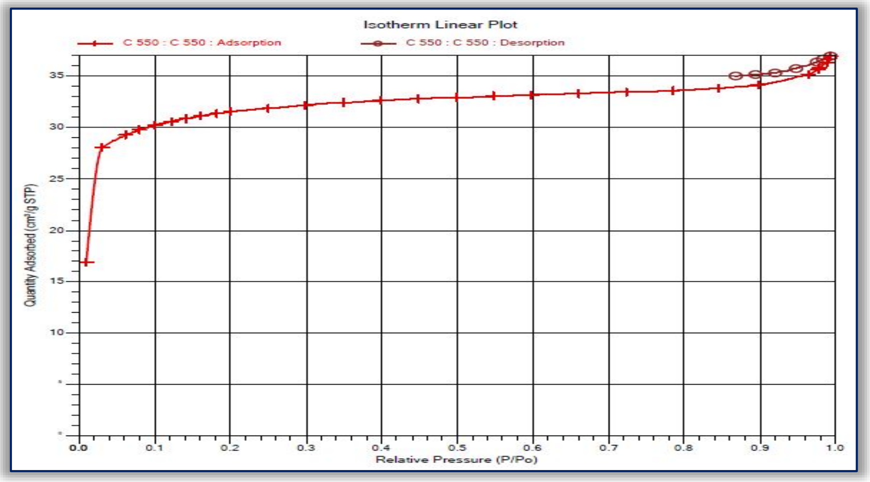

Figure 9. Isothermal Linear Plot of Activated Carbon at 550ᵒC.

Figure 10. Isothermal Linear Plot of Activated Carbon at 600ᵒC

— Particle size analysis

Particle size analysis, particle size measurement, or simply particle sizing is the collective name of the technical procedures, or laboratory techniques which determines the size range and/or the average size of the particles in a powder sample. From the particle size distribution graph at d(0.1) is the diameter of the particle at which 10% of the sample mass comprised of particles with a diameter smaller than 27.651 µm. The d(0.5) is the diameter of the particle at which 50% of the sample's mass comprised of particles with smaller than 218.900 µm. The d(0.9) is the diameter of the particle in which 90% of sample mass comprised of particle which is smaller than 771.434 µm Figure [11–13]. From the tabular data Figure [14–16] particle size of 275.423 µm is containing highest 5.12% Volume for 550ᵒC. [9,11].

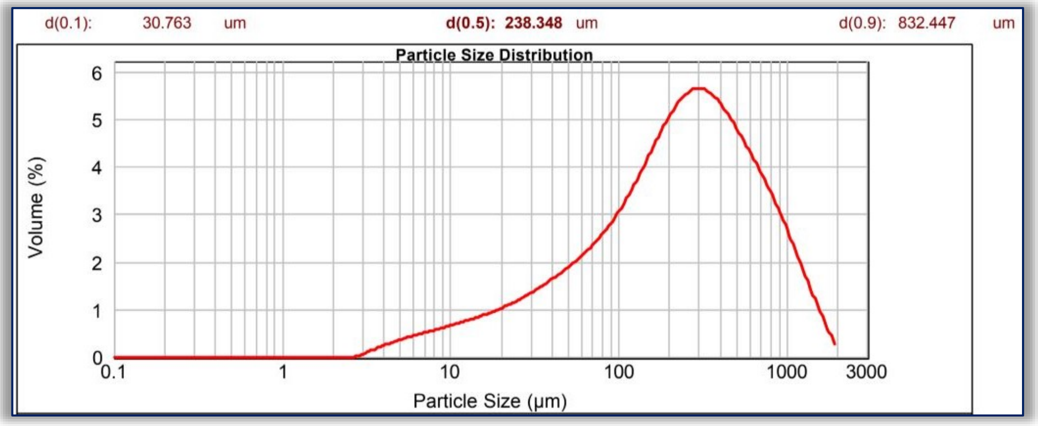

Figure 11. Particle Size Distribution Graph of Activated Carbon at 500ᵒC

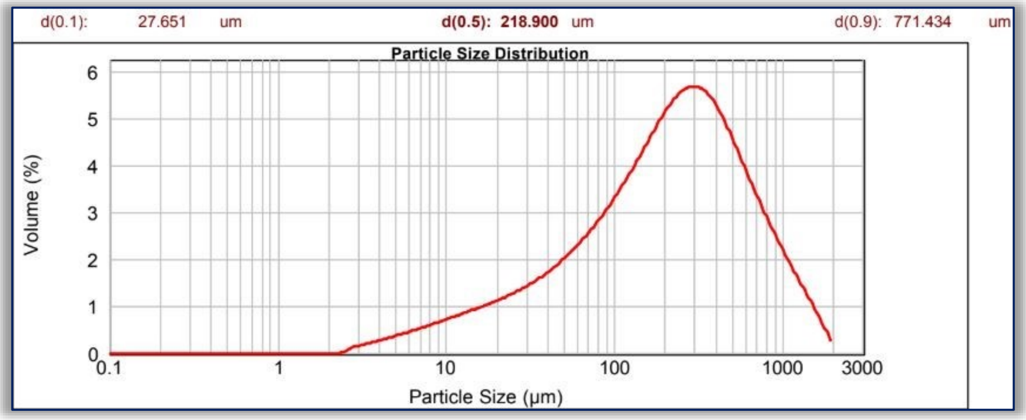

Figure 12. Particle Size Distribution Graph of Activated Carbon at 550°C

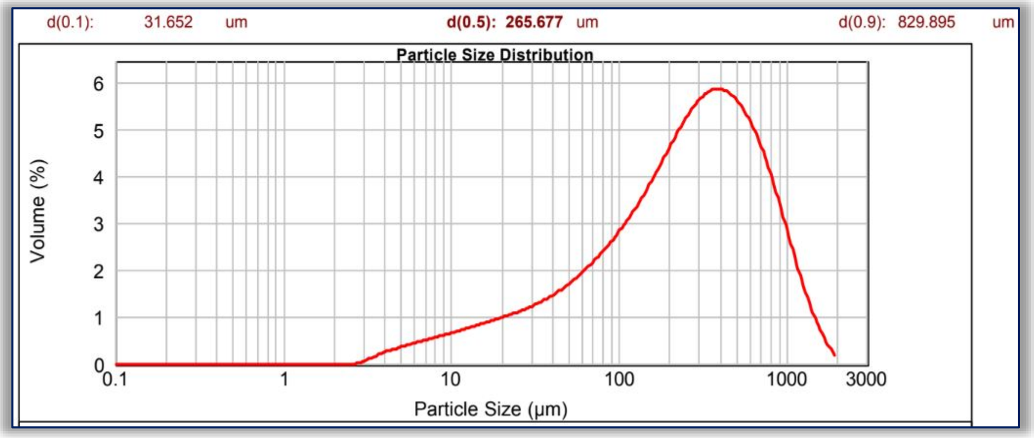

Figure 13. Particle Size Distribution Graph of Activated Carbon at 600°C

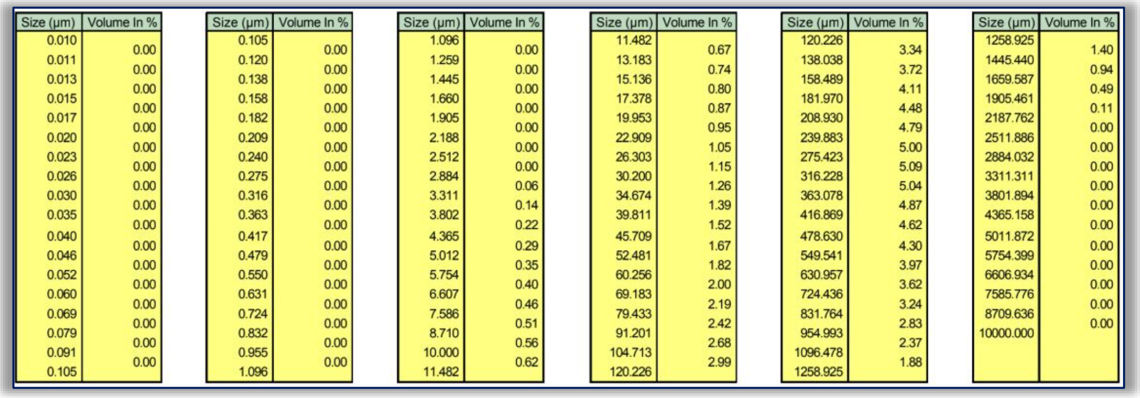

Size (μm)	Volume In %	Size (μm)	Volume In %	Size (μm)	Volume In %	Size (μm)	Volume In %	Size (μm)	Volume In %	Size (μm)	Volume In %
0.010	0.00	0.105	0.00	1.096	0.00	11.482	0.67	120.226	3.34	1258.925	1.40
0.011	0.00	0.120	0.00	1.259	0.00	13.183	0.74	138.038	3.72	1445.440	0.94
0.013	0.00	0.138	0.00	1.445	0.00	15.136	0.80	158.489	4.11	1659.587	0.49
0.015	0.00	0.158	0.00	1.660	0.00	17.378	0.87	181.970	4.48	1905.461	0.11
0.017	0.00	0.182	0.00	1.905	0.00	19.953	0.95	208.930	4.79	2187.762	0.00
0.020	0.00	0.209	0.00	2.188	0.00	22.909	1.05	239.883	5.00	2511.886	0.00
0.023	0.00	0.240	0.00	2.512	0.00	26.303	1.15	275.423	5.09	2884.032	0.00
0.026	0.00	0.275	0.00	2.884	0.06	30.200	1.26	316.228	5.04	3311.311	0.00
0.030	0.00	0.316	0.00	3.311	0.14	34.674	1.39	363.078	4.87	3801.894	0.00
0.035	0.00	0.363	0.00	3.802	0.22	39.811	1.52	416.869	4.62	4365.158	0.00
0.040	0.00	0.417	0.00	4.365	0.29	45.709	1.67	478.630	4.30	5011.872	0.00
0.046	0.00	0.479	0.00	5.012	0.35	52.481	1.82	549.541	3.97	5754.399	0.00
0.052	0.00	0.550	0.00	5.754	0.40	60.256	2.00	630.957	3.62	6606.934	0.00
0.060	0.00	0.631	0.00	6.607	0.46	69.183	2.19	724.436	3.24	7585.776	0.00
0.069	0.00	0.724	0.00	7.586	0.51	79.433	2.42	831.764	2.83	8709.636	0.00
0.079	0.00	0.832	0.00	8.710	0.56	91.201	2.68	954.993	2.37	10000.000	
0.091	0.00	0.955	0.00	10.000	0.62	104.713	2.99	1096.478	1.88		
0.105		1.096		11.482		120.226		1258.925			

Figure 14. Size to Volume Distribution Table of activated carbon at 500°C

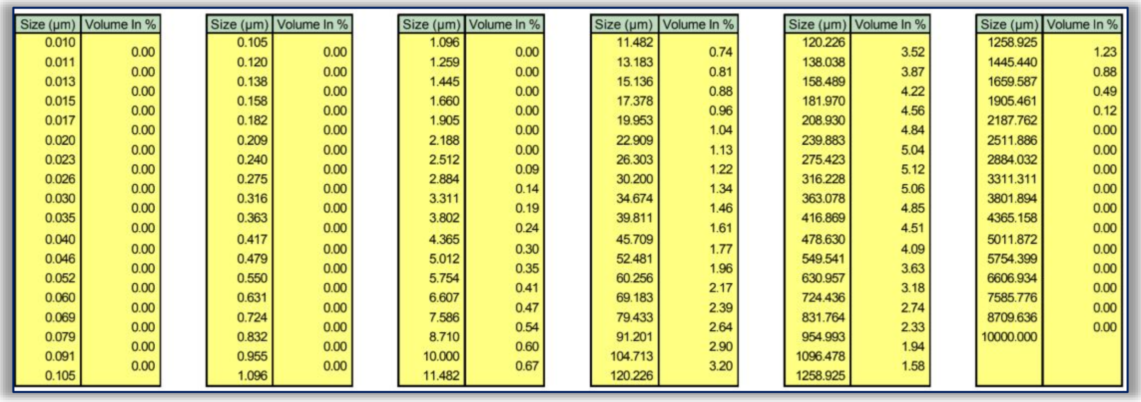

Size (μm)	Volume In %	Size (μm)	Volume In %	Size (μm)	Volume In %	Size (μm)	Volume In %	Size (μm)	Volume In %	Size (μm)	Volume In %
0.010	0.00	0.105	0.00	1.096	0.00	11.482	0.74	120.226	3.52	1258.925	1.23
0.011	0.00	0.120	0.00	1.259	0.00	13.183	0.81	138.038	3.87	1445.440	0.88
0.013	0.00	0.138	0.00	1.445	0.00	15.136	0.88	158.489	4.22	1659.587	0.49
0.015	0.00	0.158	0.00	1.660	0.00	17.378	0.96	181.970	4.56	1905.461	0.12
0.017	0.00	0.182	0.00	1.905	0.00	19.953	1.04	208.930	4.84	2187.762	0.00
0.020	0.00	0.209	0.00	2.188	0.00	22.909	1.13	239.883	5.04	2511.886	0.00
0.023	0.00	0.240	0.00	2.512	0.09	26.303	1.22	275.423	5.12	2884.032	0.00
0.026	0.00	0.275	0.00	2.884	0.14	30.200	1.34	316.228	5.06	3311.311	0.00
0.030	0.00	0.316	0.00	3.311	0.19	34.674	1.46	363.078	4.85	3801.894	0.00
0.035	0.00	0.363	0.00	3.802	0.24	39.811	1.61	416.869	4.51	4365.158	0.00
0.040	0.00	0.417	0.00	4.365	0.30	45.709	1.77	478.630	4.09	5011.872	0.00
0.046	0.00	0.479	0.00	5.012	0.35	52.481	1.96	549.541	3.63	5754.399	0.00
0.052	0.00	0.550	0.00	5.754	0.41	60.256	2.17	630.957	3.18	6606.934	0.00
0.060	0.00	0.631	0.00	6.607	0.47	69.183	2.39	724.436	2.74	7585.776	0.00
0.069	0.00	0.724	0.00	7.586	0.54	79.433	2.64	831.764	2.33	8709.636	0.00
0.079	0.00	0.832	0.00	8.710	0.60	91.201	2.90	954.993	1.94	10000.000	
0.091	0.00	0.955	0.00	10.000	0.67	104.713	3.20	1096.478	1.58		
0.105		1.096		11.482		120.226		1258.925			

Figure 15. Size to Volume Distribution Table of activated carbon at 550°C

Size (µm)	Volume In %	Size (µm)	Volume In %	Size (µm)	Volume In %	Size (µm)	Volume In %	Size (µm)	Volume In %	Size (µm)	Volume In %
0.010	0.00	0.105	0.00	1.096	0.00	11.482	0.67	120.226	3.03	1258.925	1.23
0.011	0.00	0.120	0.00	1.259	0.00	13.183	0.73	138.038	3.36	1445.440	0.74
0.013	0.00	0.138	0.00	1.445	0.00	15.136	0.79	158.489	3.71	1659.587	0.35
0.015	0.00	0.158	0.00	1.660	0.00	17.378	0.85	181.970	4.08	1905.461	0.08
0.017	0.00	0.182	0.00	1.905	0.00	19.953	0.92	208.930	4.44	2187.762	0.00
0.020	0.00	0.209	0.00	2.188	0.00	22.909	0.98	239.883	4.77	2511.886	0.00
0.023	0.00	0.240	0.00	2.512	0.00	26.303	1.06	275.423	5.04	2884.032	0.00
0.026	0.00	0.275	0.00	2.884	0.06	30.200	1.14	316.228	5.22	3311.311	0.00
0.030	0.00	0.316	0.00	3.311	0.14	34.674	1.25	363.078	5.29	3801.894	0.00
0.035	0.00	0.363	0.00	3.802	0.23	39.811	1.36	416.869	5.24	4365.158	0.00
0.040	0.00	0.417	0.00	4.365	0.29	45.709	1.50	478.630	5.06	5011.872	0.00
0.046	0.00	0.479	0.00	5.012	0.35	52.481	1.66	549.541	4.76	5754.399	0.00
0.052	0.00	0.550	0.00	5.754	0.40	60.256	1.84	630.957	4.35	6606.934	0.00
0.060	0.00	0.631	0.00	6.607	0.46	69.183	2.03	724.436	3.82	7585.776	0.00
0.069	0.00	0.724	0.00	7.586	0.51	79.433	2.25	831.764	3.20	8709.636	0.00
0.079	0.00	0.832	0.00	8.710	0.56	91.201	2.48	954.993	2.51	10000.000	
0.091	0.00	0.955	0.00	10.000	0.61	104.713	2.75	1096.478	1.84		
0.105		1.096		11.482		120.226		1258.925			

Figure 16. Size to Volume Distribution Table of activated carbon at 600°C

— FESEM (Field Emission Scanning Electron Microscope)

Field emission scanning electron microscopy (FESEM) provides topographical and elemental information at magnifications of 10x to 300,000x, with virtually unlimited depth of field.

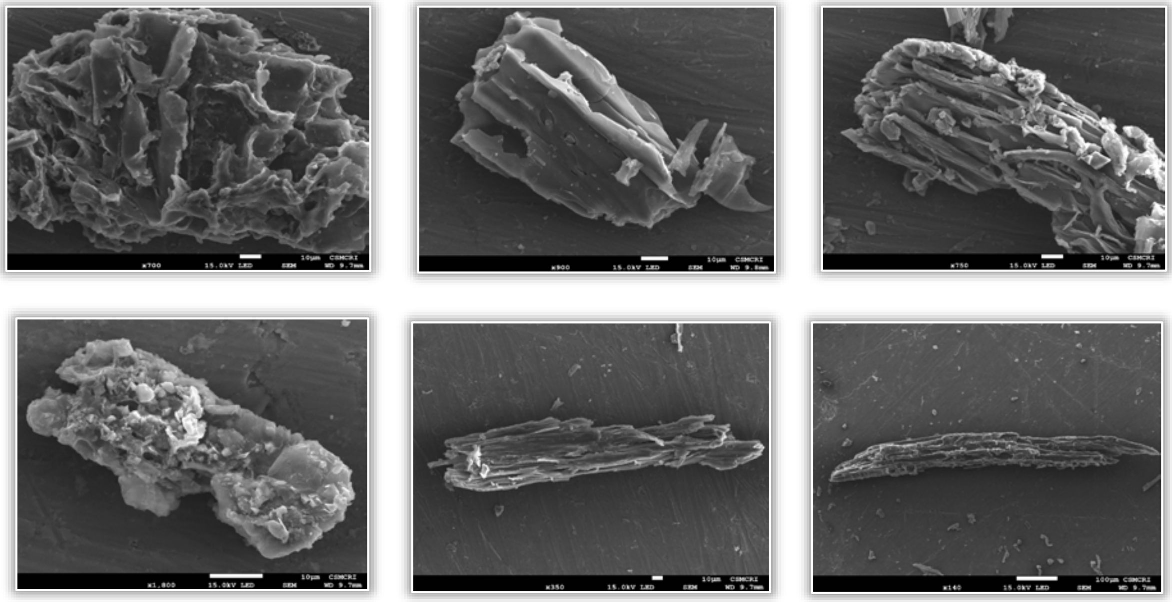

Figure 17. FE–SEM (Field Emission Scanning Electron Microscope) Image of Activated Carbon at 500°C

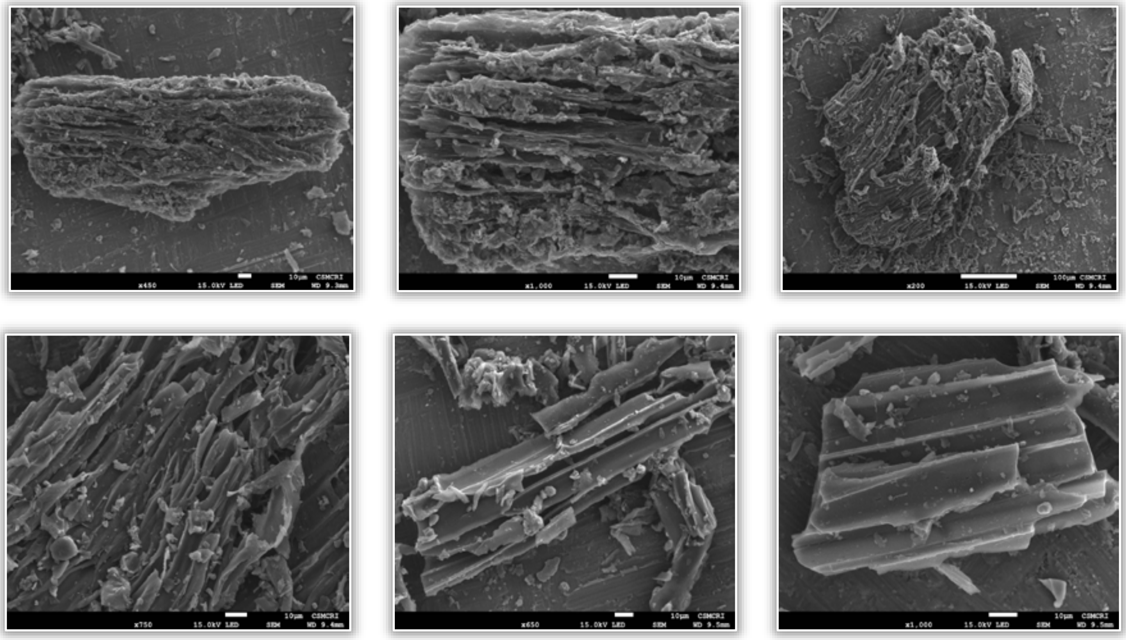

Figure 18. FE–SEM (Field Emission Scanning Electron Microscope) Image of Activated Carbon at 550°C

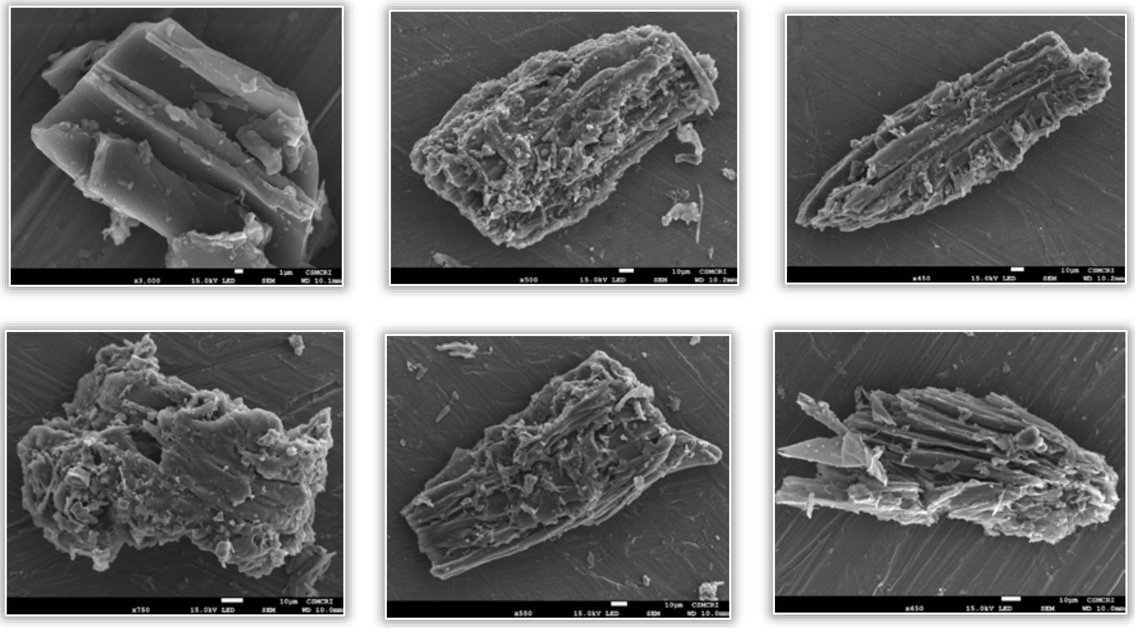

Figure 19. FE–SEM (Field Emission Scanning Electron Microscope) Image of Activated Carbon at 600°C

Compared with convention scanning electron microscopy (SEM), field emission SEM (FESEM) produces clearer, less electro statically distorted images with spatial resolution down to 1 nanometers – three to six times better. Figure [17–19] shows the result of FESEM for the sample reading of three different temperatures (500°C, 550°C and 600°C) [16,17].

4. CONCLUSIONS

Generally BET surface area range is from 500–1500 m^2/g and pore volume is 0.3–0.8 cm^3/g. The Resultant product BET Surface Area shows that at 550°C the highest surface area of activated carbon is 969.075 m^2/g. and pore volume is 0.5 cm^3/g. Elemental Analysis also shows higher value of % Fixed carbon content in to the product if it is heated at 550°C as compare to other temperature range. By studying and comparing characterization like Elemental Analysis, Powder XRD, Surface Area – Porosity Measurement (BET), Particle Size Analysis and FESEM, activated carbon produced from Pinewood with the help of pyrolysis process at 550°C temperature has given a satisfactory result. Hence activated carbon prepared from Pinewood can be effectively used for the removal of pollutants from wastewaters.

Acknowledgements

The authors thankfully acknowledge Process Design and Engineering Division, CSMCRI (Central Salt and Marine Chemicals Research Institute), Bhavnagar for the technical support.

References

[1] Musa Mutah, Kikuchi Akira, Abdul Majid Zaiton, Jaafar Jafariah, Salim Mohd Razman, Ismail Nor Eman, Production of sugarcane bagasse based activated carbon for Cd2+ removal using factorial design. International Journal of Innovative Technology and Exploring Engineering (IJITEE) 2(4), 2013, 121–125

[2] Verla, A.W, M. Horsfall (Jnr), E.N Verla, A.I. Spiff, O.A. Ekpete, Preparation and characterization of activated carbon from Fluted pumpkin seed shell. Asian Journal of Natural and Applied Sciences; 1(3), 2012, 39–50

[3] Aura Marina Hernández, Mary Labady, Jorge Laine, Granular activated carbon from wood originated from tropical virgin forest, Open Journal of Forestry, 4, 2014, 208–211

[4] Ramakrishna Gottipati, Preparation and characterization of micro porous activated carbon from biomass and its application in the removal of Chromium (VI) from aqueous phase. Phd. Thesis, 2012, 1–217

[5] Billy T H Guan, Puziah Abdul Latif, Taufiq Y H, Physical preparation of activated Carbon from sugarcane bagasse and corn husk and its physical and chemical characteristics. International Journal of Engineering Sciences & Research Technology 2(3),2013, 1–14

[6] C.S. Ajinomoh, Nurudeen Salahudeen, Production of activated carbon from sugar cane bagasse, Australian Journal of Industry Research, SCIE Journals, 16–22

[7] S. Dinesh, Development and characterization of pellet activated carbon from new precursor, phd. Thesis, 2011, 1–54

[8] Siti Khadijah C.O., Siti Fatimah C.O, N Aina Misnon, F. Hanim K, Development and characterization of pellet activated carbon from new precursor. International Journal of Engineering and Applied Sciences, 2012. Vol. 1, No.2, 76–85

[9] Khezami, A. Chetouani, B. Taouk, R. capart, Production and characterization of activated carbon from wood components in powder. Powder technology 157 (2005), 48–56

[10] J. Rizhikovs, J. Zandersons, B.Spince, G. Dobele, E. Jakab, Preparation of granular activated carbon from hydrothermally treated and pelletized deciduous wood. Journal of analytical and applied pyrolysis 93 (2012), 68–76
[11] Sait Yorgun, Derya Yildiz. Preparation and characterization of activated carbons from paulownia wood by chemical activation with H3P04. Journal of the Taiwan Institute of Chemical Engineers 001 (2015) 1–10
[12] Gyung Goo Choi, Seung Jin Oh, Soon Jang Lee, Joo Sik Kim, Production of bio–based phenolic resin and activated carbon from bio–oil and biochar derived from fast pyrolysis of palm kernel shells, Bioresource Technology, 178 (2015) 99–107
[13] Charles M. Cali, Taiying Zhang, Rajeev Kumar, Charles E. Wyman, solvent systems for enhanced furfural and hydroxymethyl furfural (HMF) production from cellulosic biomass, Sun Grant National Conference, New Orleans, Louisiana, 2012
[14] Praveen Kumar, Diane M. Barrett, Micheal J. Delwiche, Pieter Stroeve, Methods of pretreatment of lignocellulosic biomass for efficient hydrolysis and biofuel production, ACS publication, 2009.
[15] Nathan Mosier, Charles Wyman, Bruce Dale, Richard Elander, Y.Y. Lee, Mark Holtzapple, Michael Ladisch, Features of promo sing technologies for pretreatment of lignocellulosic biomass, ELSEVIER publication, 2005, 673–686
[16] P.H. Groggins, Unit processes in organic synthesis., fifth addition, Tata McGraw– Hill publication, 775 – 777, 2004
[17] Shuntaro Tsubaki, Junichi Azuma, Application of microwave technology for utilization of recalcitrat biomass, Division of Environmental Science, Graduate School of Agriculture, Kyoto University Japan, 667 – 722, 2011.
[18] Adina–Elena Segneanu, Florentina Cziple, Paulina Vlazan, Paula Sfirloaga, Ioan Grozescu, Vasile Daniel Gherman, Biomass Extraction Methods, Biomass Now – Sustainable Growth and Use , Page No. 389–400,2013
[19] Luxin Zhang, Hongbing yu, Pan Wang, Solid acid as catalysts for the conversion of D–xylose, xylan and lignocellulosic into furfural in ionic liquid, Science Direct – Elsevier Bioresource Technology – Vol.136 (2013) 515–521
[20] Junhua Zhang, Junping Zhuang, Lu Lin, Shijie Liu, Zhuo Zhang, Conversion of D–xylose into furfural with Mesopores molecular sieve MCM–41 as catalyst and butanol as the extraction phase, Science Direct – Elsevier Bioresource Technology – (2012), 73–77
[21] Luxin Zhang, hongbing yu, Pan Wang, Heng dong, Xinhong Peng, Conversion of xylan, D–xylose and lignocellulosic biomass into furfural using AlCl3 as catalyst in ionic liquid, Science Direct – Elsevier Bioresource Technology – Vol.130 (2013), 110–116
[22] K. Dussan, B. Girisuta, D. Haverty, J.J. Leahy, M.H.B. Hayes, Kinetics of levulinic acid furfural production from Miscanthus * giganteus, Science Direct – Elsevier Bioresource Technology – Vol.149(2013), 216–224
[23] 6.B.Girisuta, B. Danon, R. Manurung, L. P.B.M. Jassen, H. J. Heeres, "Experimental and kinetic modeling studies on the acid– catalyzed hydrolysis of the water hyacinth plant to levulinic acid", Science Direct – Elsevier Bioresource Technology – Vol. 99(2008), 8367–8375.
[24] Zeh Zhan, Zongbao k.Zhao, Microwave–assisted conversion of lignocellulosic biomass into furans in ionic liquid, Science Direct – Elsevier Bioresource Technology –Vol. 101(2010), 1111–1114.
[25] Feng Guo, Zhen Fang, Tie–jun Zhou, Conversion of fructose and glucose into 5–hydroxymethylfurfural with lignin–derived carbonaceous catalyst under microwave irradiation in dimethyl sulfoxide–ionic liquid mixtures, Science Direct – Elsevier Bioresource Technology – (2012), 1–6.
[26] Galletti et al., Levulinic acid from waste biomass, Bio Resources, Vol. 7–2 (2012), 1824–1835.
[27] Gianluca Marcotullio, Furfural production in modern lignocellulosic – feed stock biorefinerires, UNECE / FAO Workshop. St. Petersburg date, 22– 24/05/2013
[28] Artur Malinowski, Dorota Wardzinska, Catalytic conversion of furfural towards fuel biocomponents, CHEMIK –Vol. 66–9 (2012), 982–990
[29] V.U. Ambalkar, Mohd. I. Talib. Synthesis of furfural from lignocellulosic biomass as agricultural residues: A Review. The International Journal of Engineering and Science (IJES) – Vol 1 (2012) 30–36
[30] Saikat Dutta, Supita De, Basudeb Saha, Md. Imteyaz Alam. Advances in conversion of hemi cellulosic biomass to furfural and upgrading to biofuels, Catalysis Science and Technology – Vol.2 (2012), 2025–2036
[31] Josefine Cragnell, Kristina Green, Andre Holmberg, Magnus Karlsson, Evaluation of processes for conversion of biomass – to – fuels using biochemical versus thermo – chemical processes, Lund Institute of technology, 2009 1–53.

ANNALS of Faculty Engineering Hunedoara – International Journal of Engineering
ISSN 1584 ~ 2665 (printed version); ISSN 2601 ~ 2332 (online); ISSN-L 1584 ~ 2665

Faculty of Engineering Hunedoara,
5, Revolutiei, 331128, Hunedoara, ROMANIA
http://annals.fih.upt.ro